Infrared absorption and the loss function of the high-T_c superconductors

S. M. Bose
Department of Physics and Atmospheric Science, Drexel University, Philadelphia, Pennsylvania 19104

P. Longe
Institut de Physique, B5, Université de Liège, Sart-Tilman, B-4000 Liège, Belgium
(Received 18 November 1992)

The loss-function tensor associated with the infrared absorption spectra of the high-T_c superconductors has been calculated. The model used is a system of layered two-dimensional electron gases where the charge carriers interact via an effective potential mediated by intra- and interlayer exchange of acoustic and optical plasmons. The calculations are applied to $La_{1.85}Sr_{0.15}CuO_4$ where the loss function has recently been obtained from careful measurements of the infrared absorption spectra. The shape of the calculated loss function is in good agreement with the experimental curve. The observed peak occurring at a frequency about 1.5 times the optical plasmon frequency is shown to correspond to the excitation of a plasmon coupled with electron-hole pairs. This theory also allows for establishment of relations between various physical parameters.

I. INTRODUCTION

In the past several years considerable attention has been paid to the optical and electron spectroscopies[1–4] of layered high-T_c cuprates with a view to obtaining information on the electronic structure and understanding the mechanism of their superconductivity. In particular, the loss function of these superconductors has been obtained from the measurements of their infrared (IR) absorption[1,2] and electron-energy-loss[3] measurements.

The loss functions obtained from the IR absorption measurements universally show an increasing slope on the low-frequency side of the spectra and a sharp maximum at a finite frequency. The slope has been reported to be quadratic by some authors, and the peak frequency has been associated with the optical plasmon frequency. In order to explain the experimental data, in this paper we present a calculation of the IR absorption spectra of a multilayered system which represents a high-T_c cuprate superconductor.

The aim of this calculation is to emphasize the possible effect of the plasmon excitation in a multilayered system on the IR spectra. Using the previously calculated effective interaction[5,6] between the charge carriers (electrons or holes, hereafter referred to as "electrons") due to intra- and interlayer exchanges of plasmons, the IR absorption spectra has been calculated and it is found that the peak can be attributed to the excitation of an optical plasmon, and the low-frequency behavior is related to the acoustic plasmons. Our calculation shows that the peak does not occur exactly at the optical plasmon frequency, but at ~ 1.5 times that frequency. Moreover, we find that the increasing slope in the loss function is quasiquadratic at low but finite frequencies and linear at very low frequencies.

In our theory the electrons in each layer of the multilayered system are assumed to form a two-dimensional electron gas (2DEG), and the IR spectra are calculated for various geometries (i.e., direction of the incident beam with respect to the layer planes and direction of the polarization vector), using the diagrammatic methods. It should be pointed out that because of the anisotropy of the layered electron system, the dielectric function $\varepsilon(Q,\omega)$ appearing in the loss function must be considered to be a tensor.

It should also be emphasized that the situation here is different from the IR absorption in an isotropic system,[7] such as an ordinary metallic 3D electron gas, where a *single* plasmon cannot be excited by the absorption of a photon, since the plasmon and photon are longitudinal and transverse excitations, respectively. The plasmon excitation has to be accompanied by some other excitation, like an electron-hole pair excitation, which shares its momentum with the plasmon in such a way that the total momentum of this plasmon-pair system is practically zero (i.e., equal to the momentum Q of the absorbed photon). For an anisotropic system, such as a multilayered electron gas, the situation is different. The transverse effective mass of the electrons being considered as very large (infinite in our model), direct single-plasmon excitation becomes, in principle, possible. However, for certain geometries, such as an IR irradiation normal to the layer planes, such single-plasmon excitations are not possible because of the symmetry of the process, and these are the precise geometries that the experimentalists have considered so far. This means that for normal incidence experiments, the situation becomes similar to that encountered in isotropic systems[7] where the plasmon has to be accompanied by a pair. The observed peak is then essentially related to a plasmon-pair system and its frequency must be higher than the frequency of an isolated plasmon.

In Sec. II, we present the theory for the IR loss function and show how the results can be obtained by using the diagrammatic techniques of the many-body perturbation theory. In Sec. III, the results of our theory are de-

0163-1829/93/48(9)/6632(7)/$06.00

scribed and compared with the currently available experimental data.

II. DIAGRAMS DESCRIBING THE IR LOSS FUNCTION

In our calculation, which is related to a radiative IR absorption process, the usual scalar loss function $\mathrm{Im}(-\varepsilon^{-1})$ has to be replaced by a more general loss function $\mathrm{Im}(\mathbf{U}\cdot\varepsilon^{-1}\cdot\mathbf{U})$, where ε^{-1} is the inverse dielectric tensor and $\mathbf{U}$ the unit polarization vector. This loss function can be written as

$$\mathrm{Im}(\mathbf{U}\cdot\varepsilon^{-1}\cdot\mathbf{U})=[v(\mathbf{Q})/\varepsilon_0]\mathrm{Im}\mathbf{R}_U(\mathbf{Q},\omega)\ , \tag{1}$$

ω and $\mathbf{Q}$ being the photon energy and momentum, respectively, and ε_0 an isotropic background dielectric function. The potential $v(\mathbf{Q})$ is the Coulomb potential $v(\mathbf{Q})=4\pi e^2/\varepsilon_0 Q^2$ ($\hbar=1$) for an isotropic system, and

$$\mathrm{Im}\mathbf{R}_U(\mathbf{Q},\omega)=(\pi/\Omega)\sum_f |\langle f|O|0\rangle|^2\delta(\mathcal{E}_f-\mathcal{E}_0-\omega) \tag{2}$$

is the response of the conduction electron system to the electromagnetic radiation represented by the operator

$$O=\sum_{n=1}^{N}\exp(i\mathbf{Q}\cdot\mathbf{X}_n)\mathbf{U}\cdot\mathbf{P}_n/mc\ . \tag{3}$$

This system occupies a volume Ω and is treated as an interacting many-body system; $|0\rangle$ and $|f\rangle$ are its initial (ground) and final states, with $\mathcal{E}_0$ and $\mathcal{E}_f$ as respective energies; the $\mathbf{X}_n$'s and the $\mathbf{P}_n$'s are the positions and momenta of the N electrons and m their *effective* mass. Note that if we had considered the response to the scalar potential of an incoming charged particle, the factor $\mathbf{U}\cdot\mathbf{P}_n/mc$ would then be missing in (3) and only the diagonal element in (1) would appear in the description of the loss (or absorption) process. The present radiative loss function will thus depend on ω and the directions of $\mathbf{Q}$ and $\mathbf{U}$.

A diagrammatic analysis of the propagator (2) shows that it can be represented by the diagrams of Fig. 1 where the solid dots are related to operators O and $O^\dagger$, i.e., to the radiative interaction, and the dashed line is related to the plasmon excitation. The dashed line could also represent multiple pair excitations contributing to the background of the IR spectrum, but in the present paper we concentrate essentially on the plasmon excitation in a multilayered system. This excitation, if isolated, would contribute as a peak (δ function). The diagrams of Fig. 1 thus represent a first-order expansion in the plasmon excitation. Note that the zeroth-order diagram is not present in the figure since it does not contribute. Indeed a *low*-energy photon cannot excite one single free electron-hole pair due to the failure of the energy-momentum conservation requirement. The fact that the final states of (2) cannot be those of a single pair means that any cut through the diagrams of Fig. 1 (by which the final states can be visualized) must also cut across the plasmon (dashed) line, which implies that only the real part of the plasmon propagator (with positive energy) has to be taken into consideration. This cut, however, may also go across either one or two additional electron-hole pair lines, depending on the topology of the diagrams. In our calculations we neglect all terms corresponding to more than one electron-hole pair in the final state because of their negligible contribution. Apart from these restrictions, any topology of the diagrams of Fig. 1 is included in our calculation. Such a diagrammatic approach was used by Tzoar and Klein[7] for the treatment of optical absorption by metals, where the conduction electrons were treated as an isotropic 3D system.

The details of our calculations are given in the Appendix. In the next section we present and discuss some of the important results of our calculation.

III. RESULTS AND DISCUSSION

The loss function resulting from our calculation can be written as

$$\mathrm{Im}(-\mathbf{U}\cdot\varepsilon^{-1}\cdot\mathbf{U})=(\pi/2\varepsilon_0)(\omega_p^0/\omega)^4\omega\delta(\omega-\omega_p^0\cos\alpha)\sin^2\alpha\sin^2\beta+(1/\pi\varepsilon_0)(\omega_p^0/\omega)^4 A(\omega)\cos^2\beta\ , \tag{4}$$

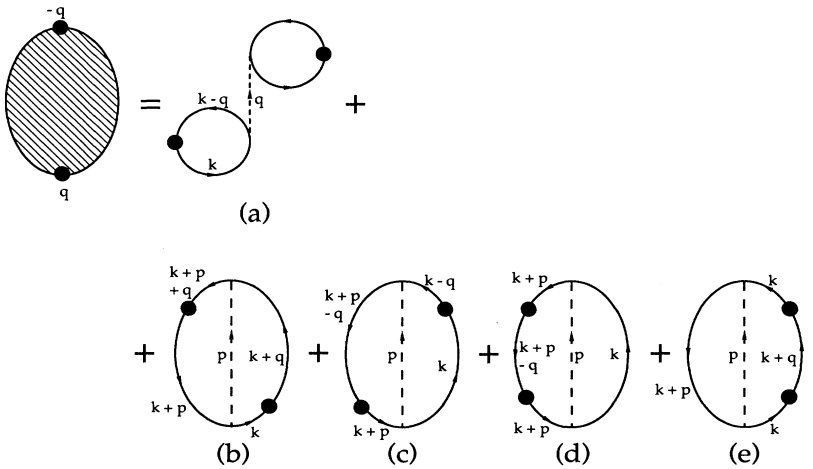

FIG. 1. Diagrammatic expansion of propagator (2). The solid dots are related to the interaction with the IR radiation and the dashed lines to the plasmon excitation.

where

$$\omega_p^0=[4\pi e^2 n_s/\varepsilon_0 ma]^{-1/2} \quad (5)$$

is the plasmon frequency, a being the interlayer distance and $n_s=k_F^2/2\pi$ the 2D electron density with k_F as the Fermi momentum. Angles α and β in (4) are between the layer planes and the wave vector, and between the layer planes and the polarization vector, respectively.

The first term on the right-hand side of (4) is the contribution of Fig. 1(a). It contains a δ function which clearly shows that Fig. 1(a) corresponds to a single plasmon and no pair in the final state (since the terms with two electron-hole pairs are negligible). To our knowledge, all the reported experiments[1,2] use a radiation with incidence normal to the layer planes. In that case $\beta=0$, and the contribution of this first term of (4) vanishes.

The second term in (4) is the total contribution of Figs. 1(b)–1(e). It contains a computed function $A(\omega)$ which presents a sharp maximum in the region $\omega\approx 1.5\omega_p^0$. As shown in the Appendix, this function is proportional to ω^5 for $\omega\ll\omega_p^0$, yielding a linear loss function for small ω. This term will contribute for all incidence angles, except for the very particular situation where the radiation is polarized and such that $\beta=90°$, and hence $\alpha=0$.

Besides the two geometrical parameters α and β, numerical evaluation of (4) requires knowledge of *four* physical parameters which characterize the high-T_c superconductors. These parameters are (i) the interlayer distance a, (ii) the areal density n_s of the electrons, (iii) their effective mass m, and (iv) the background dielectric constant ε_0. In fact, these parameters only characterize the most simple multilayered compounds, those with one interlayer spacing or, in other words one layer per cell. Strictly speaking our calculations are applicable only to those compounds, but we may consider that they can be extended to other ones, insofar as the IR wavelength $2\pi/Q$ is large compared to the details of the structure and thus cannot be revealed by IR radiation. For instance, if there are two or more spacings between adjacent layers, and if n_s depends on the position of the layer, we may consider that the IR photons will only "see" an average spacing $a_{\rm av}$ and an average 2D density $n_{s,\rm av}=n_v a_{\rm av}$. These average quantities can be introduced if we want to extend the present calculation to other compounds.

Most of the above parameters can be obtained by various experimental techniques. A particular good set of values (except for ε_0) has been presented and discussed by Kresin and Wolf[8] for $La_{1.8}Sr_{0.2}CuO_4$, a compound with only one interlayer spacing. On the other hand, Kim *et al.*[2] have plotted the loss function for this compound from their measured IR absorption spectra. We will thus pay particular attention to La-Sr-Cu-O: (i) to test our theory, (ii) to see how the loss function may vary if we modify these parameters and how sensitive it is to their choice, and (iii) to see what additional information the investigation of the IR spectra may yield, besides those obtained so far.

If the incident IR radiation is not polarized (as is the case in most experiments), one has just to replace $\sin^2\beta$ and $\cos^2\beta$ in (4) by their average values, which are $\frac{1}{2}\cos^2\alpha$ and $1-\frac{1}{2}\cos^2\alpha$, respectively. If, moreover, the radiation is normal to the layer planes, one has $\alpha=\pi/2$ and the loss function becomes

$$\mathrm{Im}(\mathbf{U}\cdot\varepsilon^{-1}\cdot\mathbf{U})=(\omega_p^0/\omega)^2 A(\omega)/2\pi\varepsilon_0\ , \quad (6)$$

where, as we have mentioned before, only Figs. 1(b)–1(e) survive. This is the loss function detected by Kim *et al.*[2]

In Fig. 2, this function (6) is plotted using the parameters proposed by Kresin and Wolf[8] for La-Sr-Cu-O, which are $a=6.6$ Å, $m/m_e=5$ (m_e being the bare electron mass), and $n_s=0.02$ Å^{-2} (obtained from $n_v=0.003$ Å$^{-3}=n_s/a$). However, these authors do not propose any value for ε_0, which will appear in our results as the only undetermined parameter. That is why in Fig. 2 we have plotted (6) choosing four different values for ε_0 varying from 1 to 5, a range which is in agreement with the generally accepted values for ε_0 for these compounds. The curves of Fig. 2 are interesting for several reasons: (i) The low-frequency part of the loss function (the part related to the acoustic plasmons) has approximately the same values from $\omega=0$ up to its maximum, regardless of the choice of ε_0. (ii) Once a choice for ε_0 is made, both

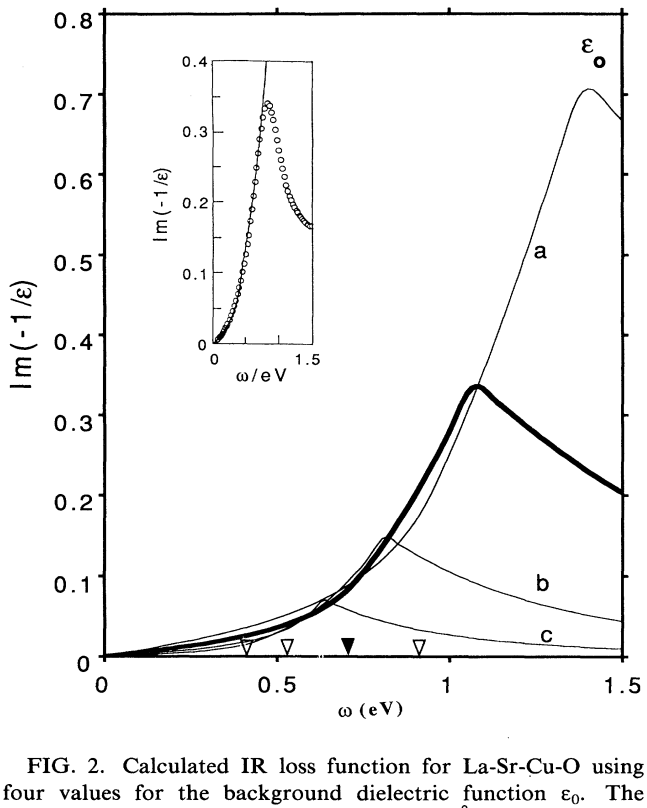

FIG. 2. Calculated IR loss function for La-Sr-Cu-O using four values for the background dielectric function ε_0. The values of the other parameters are $a=6.6$ Å, $m/m_e=5$, and $n_s=0.02$ Å^{-2} as in Ref. 8. The best fit to the experimental loss function (Ref. 2, see inset) is obtained for $\varepsilon_0=1.7$ (thick curve). The other test values of ε_0 are (*a*) 1, (*b*) 3, and (*c*) 5. The triangles indicate the frequencies taken by ω_p^0 for each ε_0. For $\varepsilon_0=1.7$, one has $\omega_p^0=0.71$ eV (solid triangle).

the position and the intensity of the maximum are fixed simultaneously. (iii) The best choice is $\varepsilon_0=1.7$, since this yields precisely those two values [$\omega=1$ eV and $\mathrm{Im}(-1/\varepsilon_0)=3.4$] presented by the experimental curve of Kim *et al.* (see the thicker curve and the inset of Fig. 2). This double "coincidence" gives much credence to our theory. More generally, it shows that, once a, m, and n_s are known for a particular sample, our theory yields a method by which its background dielectric function ε_0 can be determined. To our knowledge no precise value

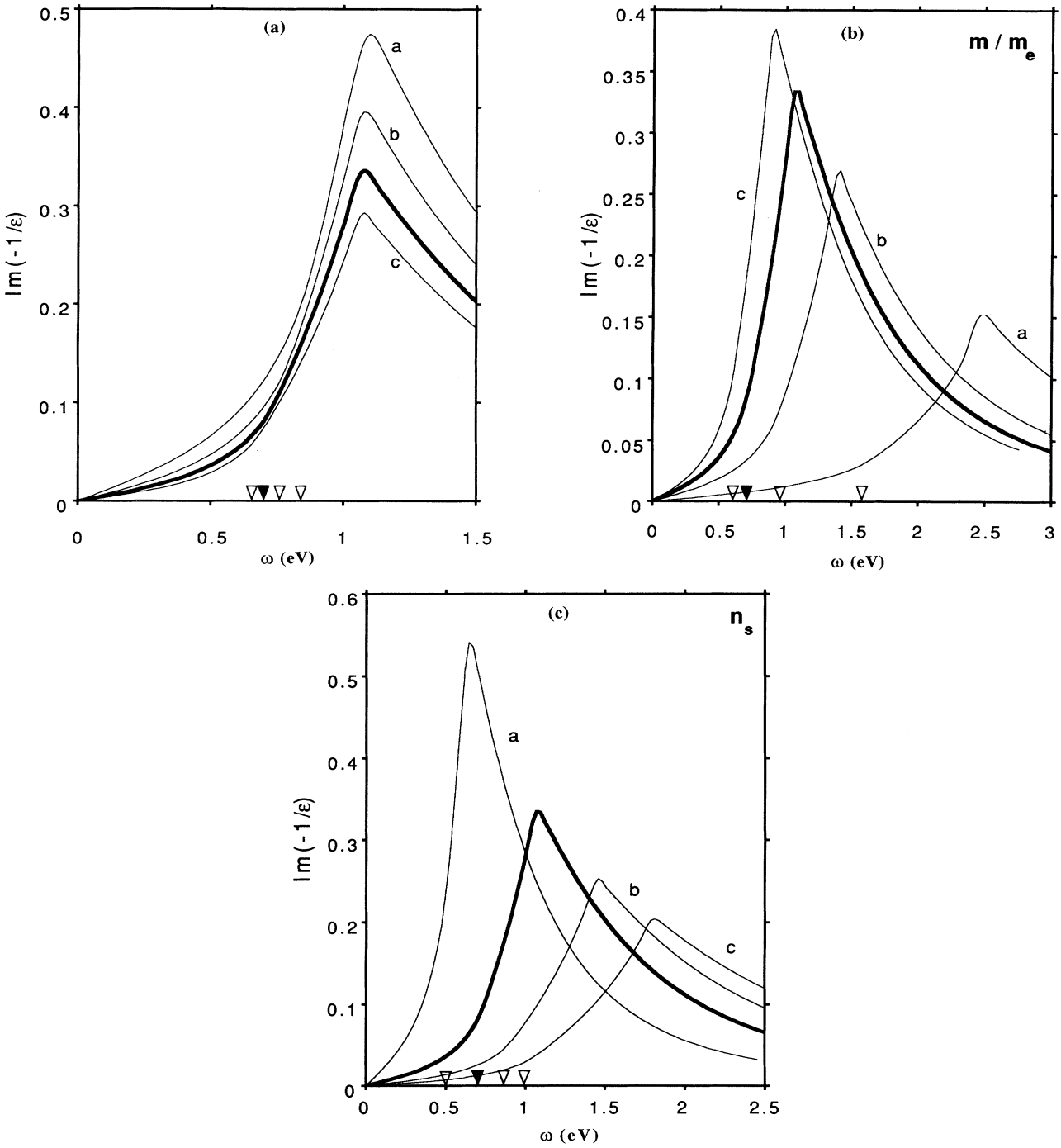

FIG. 3. In the three diagrams above, the reference (thick) curves are the same as the best fit of Fig. 2, with $\varepsilon_0=1.7$, $a=6.6$ Å, $m/m_e=5$, and $n_s=0.02$ Å^{-2}. In (a), a takes three other test values: (a) 4.6 Å, (b) 5.6 Å, and (c) 7.6 Å. In (b), m/m_e takes three other test values: (a) 1, (b) 3, and (c) 7. Finally, in the (c), n_s takes three other test values: (a) 0.01 Å^{-2}, (b) 0.03 Å^{-2}, and (c) 0.04 Å^{-2}. The triangles indicate the frequencies of ω_p^0 for each curve.

has been reported for ε_0 for La-Sr-Cu-O, but the value we propose here appears quite acceptable. (iv) We note that the general shape of our curve follows the experimental curve of Kim *et al.*[2] Indeed for small but finite values of ω, our curves have an increasing slope and are quasiquadratic, in agreement with those presented by Bozovic[1] and Kim *et al.*[2] In the Appendix we show, however, that the behavior is linear for *very* small values of ω. (v) Let us emphasize another important point. The frequency of the maximum (1 eV) in Fig. 2 is larger than the plasmon frequency $\omega_p^0=0.71$ eV obtained from (5) and indicated in Fig. 2 by a solid triangle. There is a factor of 1.55 between these two frequencies, and a factor close to this value is maintained even if we modify the values of ε_0 and/or the other parameters, as indicated by the open triangles in Figs. 2 and 3. The reason for this difference is that the peak really corresponds to the excitation of a plasmon coupled with an electron-hole pair.

Finally we have investigated the stability of our results with regard to the changes of the three other parameters. The modified curves are shown in Fig. 3 where m/m_e varies between 1 and 7, n_s between 0.01 and 0.04 Å^{-2}, and a between 4.6 and 7.6 Å. (The thick curves of Figs. 2 and 3 are all related to the same choice of parameters.) We note that any choice other than the values proposed by Kresin and Wolf[8] would destroy the double coincidence we have mentioned: no value of ε_0 would then fit the value *and* the position of the maximum, *together* and so closely with the experimental results of Kim *et al.*[2]

ACKNOWLEDGMENTS

This work was partially supported by the NATO Research Grant No. CRG 910966. The work of P.L. was supported by the Fonds National de la Recherche Scientifique, Belgium. His work was also partially supported by the Joint Project No. 92/159 of the Ministry of Research of the French Community of Belgium.

APPENDIX

This appendix provides some details of the calculations leading from Eq. (1) to Eq. (4). Let us first give the diagrammatic rules adapted for a multilayer system. These rules yield the factors contributing to the propagator $-i\mathbf{R}_U(\mathbf{Q},\omega)$ of an *interacting* electron-hole pair excited by a radiation field, as represented in Fig. 1, derived from the vector potential $\mathbf{U}\exp i(\mathbf{Q}\cdot\mathbf{x}-\omega t)$.

(i) To the particle lines, one associates factors $i\theta(k-k_F)/(\omega-E_k+i0)$ or $i\theta(k_F-k)/(\omega-E_k-i0)$, according to the directions "up" or "down" of these lines. The θ function is the usual step function, and one has $E_k=k^2/2m$, where k is a 2D momentum.

(ii) To a solid dot, related to the radiative interaction, one associates a factor $\mathbf{u}\cdot\mathbf{k}/mc$, $\mathbf{u}$ being the component of polarization $\mathbf{U}$ parallel to the layer planes, and $\mathbf{k}$ the momentum related to the particle line entering the dot.

(iii) To the plasmon (dashed) upward line, one associates a factor $\mathrm{Im}\mathcal{V}_+(\mathbf{P},\omega)$ which is described below.

(iv) To each bubble, one associates a spin factor -2.

(v) Integrations are performed over all internal momenta and energies, i.e., $\int d^3p/(2\pi)^3\cdots$ for the plasmon momentum, $(1/a)\int d^2k/(2\pi)^2\cdots$ for the particle momenta, and $\int d\omega/2\pi\cdots$ for the energies.

In a multilayered system, one has the random-phase approximation (RPA) potential

$$\mathcal{V}_+(\mathbf{P},\omega)=\frac{aV(\mathbf{P})}{\varepsilon_0+V(\mathbf{p})\mathrm{Re}\Pi_0(p,\omega)+i0}\ ,$$

where

$$V(\mathbf{P})=\frac{2\pi e^2}{p}\frac{\sinh ap}{\cosh ap-\cos ap_z}$$

is the Coulomb potential valid for a multilayered 2DEG system[5,6] and $\Pi_0(p,\omega)$ the noninteracting pair propagator inside a 2DEG; $\mathbf{p}$ and p_z are the components of $\mathbf{P}$ parallel and perpendicular to the layer planes, respectively. One has

$$\mathrm{Re}\Pi_0(p,\omega)=-n_sp^2/m\omega^2$$

as long as p is of the order or smaller than k_F. From the above expressions, one obtains

$$\mathrm{Im}\mathcal{V}_+(\mathbf{P},\omega)=-\pi v(p)F(\mathbf{P})\delta[1-(\omega_p/\omega)^2F(\mathbf{P})] \tag{A1}$$

with $v(p)=4\pi e^2/\varepsilon_0p^2$ and

$$F(\mathbf{P})=\frac{ap}{2}\frac{\sinh ap}{\cosh ap-\cos ap_z}\ . \tag{A2}$$

Note that expression (A1) for $\mathrm{Im}\mathcal{V}_+$ is the same as that for an isotropic 3D electron system, except for the occurrence of function $F(\mathbf{P})$.

Let us now use the above rules and expressions to calculate propagator $-i\mathbf{R}_U(\mathbf{Q},\omega)$ appearing in the diagrams of Fig. 1, and then calculate the loss function given by (1). First let us consider Fig. 1(a), even though this diagram does not contribute to the loss function when the incidence of radiation is normal to the layer planes, as in all experiments reported in Refs. 1 and 2.

Using the above rules, one obtains

$$[-\mathbf{R}_U(\mathbf{Q},\omega)]_a=[-i\mathbf{r}_U(\mathbf{q},\omega)]^2\mathrm{Im}\mathcal{V}_+(\mathbf{Q},\omega)\ , \tag{A3}$$

where the bubble contribution is given by

$$-i\mathbf{r}_U(\mathbf{q},\omega)=\frac{2i}{\omega a}\int\frac{d^2k}{(2\pi)^2}\frac{\mathbf{u}\cdot\mathbf{k}}{mc}[\theta(k_F-k)\theta(|\mathbf{k}+\mathbf{q}|-k_F)-\theta(k-k_F)\theta(k_F-|\mathbf{k}+\mathbf{q}|)]\ , \tag{A4}$$

$\mathbf{k}$ and $\mathbf{q}$ being the 2D momenta as indicated in Fig. 1(a). Note that in these equations, (A3) and (A4), we have assumed Q and $q\,(=Q\cos\alpha)$ much smaller than $k\sim 1/a$.

Introducing the following vector components parallel and perpendicular to the layer planes,

$$\mathbf{Q}=(\mathbf{q};q_z)=(Q\cos\alpha,0;Q\sin\alpha)$$

and

$$\mathbf{U}=(\mathbf{u};u_z)=(\cos\beta\cos\varepsilon,\cos\beta\sin\varepsilon;\sin\beta)$$

for the photon momentum and polarization vector, respectively, and

$$\mathbf{k}=(k\cos\phi,k\sin\phi)$$

for the particle 2D momentum, the double integration of (A4) can be performed. One obtains

$$-i\mathbf{r}_U(\mathbf{q},\omega)=\frac{ik_F^2 q}{2\pi amc\omega}\cos\beta\cos\varepsilon=\frac{-in_s}{amc^2}\sin\alpha\sin\beta\ , \tag{A5}$$

where the result of the last step is obtained using the relations $\cos\varepsilon=-\tan\alpha\tan\beta$ (since $\mathbf{U}\cdot\mathbf{Q}=0$), and $q=Q\cos\alpha=(\omega/c)\cos\alpha$.

Finally, using the fact that the arguments of $\mathrm{Im}\mathcal{V}_+(\mathbf{Q},\omega)$ in (A3) are related to the photon, we can replace $F(\mathbf{Q})$, given by (A2), by $\cos^2\alpha$, which is its small q and q_z limits, and one obtains

$$\mathrm{Im}\mathcal{V}_+(\mathbf{Q},\omega)=-\frac{2\pi^2e^2c^2}{\varepsilon_0\omega}\delta(\omega-\omega_p\cos\alpha)\ . \tag{A6}$$

Substituting (A5) and (A6) into (A3), and then (A3) into (1), one obtains the first term of (4), i.e., the contribution of Fig. 1(a).

Contributions of Figs. 1(b)–1(e) are obtained by using the above diagrammatic rules and the notations shown in Figs. 1(b)–1(e):

$$[-\mathbf{R}_U(\mathbf{Q},\omega)]_{\mathrm{(b)-(e)}}=\frac{-2}{\omega^2 a}\int\frac{d^2k}{(2\pi)^2}\int\frac{d^3p}{(2\pi)^3}\theta(k-k_F)\theta(k_F-|\mathbf{k}+\mathbf{p}|)\frac{[\mathbf{u}\cdot\mathbf{p}]^2}{m^2c^2}\mathrm{Im}\mathcal{V}_+(\mathbf{P},\tilde{\omega}) \tag{A7}$$

with

$$\tilde{\omega}=\omega-E_{|\mathbf{k}+\mathbf{p}|}+E_k\ , \tag{A8}$$

where again we have assumed that Q or q (photon momentum) is small compared to $k\sim 1/a$ (electron momentum). In fact, the factor $[\mathbf{u}\cdot\mathbf{p}]^2$ in (A7) stands for the summation of the following four terms:

$$-[(\mathbf{k}+\mathbf{p})\cdot\mathbf{u}][\mathbf{k}\cdot\mathbf{u}]-[\mathbf{k}\cdot\mathbf{u}][(\mathbf{k}+\mathbf{p})\cdot\mathbf{u}]+[(\mathbf{k}+\mathbf{p})\cdot\mathbf{u}]^2+[\mathbf{k}\cdot\mathbf{u}]^2\ ,$$

each being related to Figs. 1(b)–1(e), respectively.

The five-dimensional integral of (A7) can be reduced to a double integral which finally can be computed as a last step. The steps of the first three analytical integrations are the following. Let us write

$$\int d^3P\cdots=\oint d\phi\int_0 dpp\int_{-\pi/a}^{\pi/a}dp_z\cdots$$

and

$$\int d^2k\cdots=\int_{-k_F}^{k_F}dk_x\int dk_y\cdots\ ,$$

where the k_y axis is perpendicular to $\mathbf{p}$ (the component of $\mathbf{P}$ in the layer plane).

The k_y integral is performed first. One has

$$\int dk_y\theta(k_F-k)\theta(|\mathbf{k}+\mathbf{p}|-k_F)=2k_FR \tag{A9}$$

with

$$\begin{aligned}R&=[1-k_x^2/k_F^2]^{1/2}\quad\text{for } k_x>k_F-p\ ,\\ R&=[1-k_x^2/k_F^2]^{1/2}-[1-(k_x+p)^2/k_F^2]^{1/2}\quad\text{for } -p/2<k_x<k_F-p\ ,\\ R&=0\quad\text{for } k_x<-p/2\ .\end{aligned} \tag{A10}$$

Next, the ϕ integration gives

$$\oint d\phi[\mathbf{u}\cdot\mathbf{p}]^2=\pi u^2p^2=\pi p^2\cos^2\beta\ . \tag{A11}$$

Then we can proceed to the p_z integration using (A1) and (A2). One obtains

$$\int_{-\pi/a}^{\pi/a}dp_zF(\mathbf{P})\delta\left[1-F(\mathbf{P})\frac{\omega_p^2}{\tilde{\omega}^2}\right]=\frac{2F_0^2}{|dF/dp_z|_0} \tag{A12}$$

with

$$F_0=\tilde{\omega}^2/\omega_p^2 \ , \tag{A13}$$

$$\left|\frac{dF}{dp_z}\right|_0 = aF_0B^{1/2} \ ,$$

and

$$B=\left[\coth\frac{ap}{2}-\frac{2F_0}{ap}\right]\left[\frac{2F_0}{ap}-\tanh\frac{ap}{2}\right] . \tag{A14}$$

This latter integration introduces the step-function factor $\theta(B)$ which yields upper and lower limits to the next (numerical) p integration. It is interesting to note that these limits correspond to the optical and acoustic limits of the plasmon band, which are, respectively, given by the dispersion relations

$$\omega=\omega_p\left[\frac{ap}{2}\coth\frac{ap}{2}\right]^{1/2}$$

and

$$\omega=\omega_p\left[\frac{ap}{2}\tanh\frac{ap}{2}\right]^{1/2} .$$

Finally by substituting (A9), (A11), and (A12) into (A7), and next (A7) into (1), one obtains the second term of (4), i.e., the contributions of Figs. 1(b)–1(e).

Finally we obtain the explicit expression of the function $A(\omega)$ which appears in (4). It has the form

$$A(\omega)=\frac{1}{k_F^3}\int_{-k_F}^{k_F}dk\int dp\,\theta(B)\frac{pRF_0}{B^{1/2}} .$$

This dimensionless expression depends on (A10), (A13), (A8), and (A14), and has to be integrated numerically.

The last point we want to show is the linear character of the second term of the loss function (4) for $\omega\sim 0$. Let us note that for that limit, (A14), (A13), and (A10) become

$$B\approx\left[\frac{2}{ap}\right]^2\left[F_0-\left[\frac{ap}{2}\right]^2\right] ,$$

$$F_0\approx(\omega-k_xp/m)^2/\omega_p^2 ,$$

and

$$R\approx k_p/[k_F(k_F^2-k^2)^{1/2}] ,$$

respectively. This yields

$$A(\omega)\propto\int_0^r dp\frac{p^3(t-p)^2}{[(r-p)(s+p)]^{1/2}}$$

for that part of $A(\omega)$ which depends on ω, where r, s, and t are proportional to ω. Hence, we conclude that $A(\omega)$ is proportional to ω^5 for $\omega\sim 0$, and the second term of (4) is linear.

[1]I. Bozovic, Phys. Rev. B **42**, 1969 (1990); I. Bozovic, J. H. Kim, J. S. Harris, Jr., and W. Y. Lee, *ibid.* **43**, 1169 (1991); I. Bozovic, J. H. Kim, J. S. Harris, Jr., E. Hellman, E. H. Hartford, and P. K. Chan, *ibid.* **46**, 1182 (1992).

[2]J. H. Kim, I. Bozovic, C. B. Eom, T. H. Geballe, and J. S. Harris, Jr., Physica C **174**, 435 (1991).

[3]C. Tarrio and S. E. Schnatterly, Phys. Rev. B **38**, 921 (1988); N. Nücker, H. Romberg, S. Nakai, B. Scheerer, J. Fink, Y. F. Yang, and Z. X. Zhao, *ibid.* **39**, 12 379 (1989), and references therein.

[4]P. Longe and S. M. Bose, in Proceedings of the 1992 Beijing International Conference on High-T_c Superconductivity, edited by Z. X. Zhao, Z. Z. Gan, and R. S. Han (World Scientific, Singapore, to be published); P. Longe and S. M. Bose, Phys. Rev. B **47**, 11 611 (1993).

[5]S. Das Sarma and J. J. Quinn, Phys. Rev. B **25**, 7603 (1982); A. L. Fetter, Ann. Phys. (N.Y.) **88**, 1 (1974); P. B. Visscher and L. M. Falicov, Phys. Rev. B **3**, 2541 (1971).

[6]S. M. Bose and P. Longe, J. Phys.: Condens. Matter **4**, 1799 (1992).

[7]N. Tzoar and A. Klein, Phys. Rev. **124**, 1297 (1961).

[8]V. Z. Kresin and S. A. Wolf, Phys. Rev. B **41**, 4278 (1990).